



## Remarkable enhancement of the TiO<sub>2</sub> photocatalyst activity under visible light by doping sulfur for dye photodecolorization

Endang Tri Wahyuni<sup>\*1</sup>, Nyayu Shafiyah Mahira<sup>1</sup>, Novianti Dwi Lestari<sup>1</sup> & Taufik Abdillah Natsir<sup>1</sup>

<sup>1</sup>Chemistry Department, Faculty of Mathematics and Natural Sciences, Universitas Gadjah Mada Sekip Utara POB Bls 21, Yogyakarta, Indonesia

E-mail: endang\_triw@ugm.ac.id

Received 27 March 2022; accepted 12 July 2022

To enhance the photoactivity of TiO<sub>2</sub> under visible light, doping TiO<sub>2</sub> by sulfur atoms from sulfuric acid has been conducted by hydrothermal method, where the concentration of the acid is varied (25, 50, and 100 mmol/L) to obtain the doped TiO<sub>2</sub>-S with various S content. The doped photocatalysts obtained are characterized by using X-ray diffraction, ultraviolet specular reflectance spectrophotometer, Fourier transform infrared, and transmission electron microscope machines. The activity of the doped photocatalyst has been examined for Congo-red photo-decolorization under visible light, via batch experiment. The research results assigned that the doping sulfur into TiO<sub>2</sub> has successfully narrowed the gap that resulted in the remarkable enhancement of the activity under visible light in the Congo red decolorization. The enhancement is influenced by S content in the photocatalyst and the highest activity is shown by TiO<sub>2</sub>-S prepared from 50 mmol/L sulfuric acids. The efficiency of the Congo-red photo-decolorization catalyzed by TiO<sub>2</sub>-S (50) is found to be controlled by reaction time, photocatalyst weight, and solution pH. By applying 50 mg of the photocatalyst weight in 50 mL of the dye solution with pH 7, within 60 min, the highest photo-decolorization of 10 mg/L Congo-red, that is 87% could be reached.

**Keywords:** Congo-red, Doping, Sulfur, TiO<sub>2</sub>, Visible light

Congo red dyes, having a structure as seen in Fig. 1, is one of the most often azo dyes used in textile, paper, and printing industries<sup>1-5</sup>, that is always contained in the corresponding industrial wastewater. Colored river water due to the dye is recognizable even at very low concentrations and is not only unpleasant but also poses a serious risk to human health and aquatic environments<sup>3,6</sup>. Therefore it is essential to develop novel and cost-effective methods to treat these types of colored effluents. Recently, dye photodegradation methods involving •OH radicals produced from a photocatalyst material under light exposure, have received strong attention due to their simplicity and high effectiveness<sup>7-9</sup>. Through this process, the complex structure of dye can be decomposed into simpler and safer molecules without producing new waste.

TiO<sub>2</sub> is one of the photocatalysts that has attracted intensive attention since it poses high oxidation power, high stability, low cost, and non-toxic properties<sup>8-11</sup>. On the other side, TiO<sub>2</sub> has a wide energy gap ( $E_g = 3,2$  eV for anatase), allowing it to be activated only by UV light, and less active under visible light irradiation<sup>2,12</sup>. Thereby, TiO<sub>2</sub> application

under inexpensive sun irradiation is restricted, because, in the solar spectrum, the UV fraction is found at only 4 - 5%, while the visible light radiation exists at about 60%<sup>3</sup>.

An intensive effort has been focused to narrow the gap, that is by doping method, both with metal<sup>13-15</sup>, and non-metal elements<sup>10-12,16</sup>. Compared to metal elemental dopants, the non-metals are more interesting due to their smaller size allowing them to be inserted into the TiO<sub>2</sub> crystal lattice facily thus the non-metals can reduce the gap more effectively<sup>17-23</sup>. Among the non-metal dopants, the sulfur (S) element is reported to give a significant narrowing gap, due to the suitability size hence could be doped better<sup>18-20</sup>. Thereby S doping could considerably enhance the performance of the doped TiO<sub>2</sub> under visible light irradiation<sup>7,8</sup>.

In the S doping, thiourea is the commonest source of sulfur dopant<sup>8,18,19</sup>. The use of the organic molecules often results in the residual carbon left on the TiO<sub>2</sub> surface, hence decreasing the photocatalyst activity<sup>9</sup>. Thiourea replacement by sulfuric acid has been proposed and could prevent carbon residue formation<sup>20</sup>. Additionally, sulfur-doped TiO<sub>2</sub> preparation is frequently carried out by sol-gel

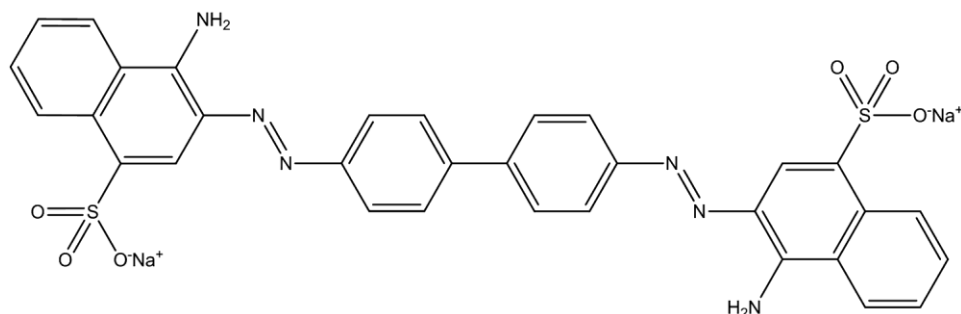


Fig. 1 — Chemical structure of Congo-red dye.

method using titanium tetraisopropoxide (TTIP) as  $\text{TiO}_2$  precursor, which is more expensive. The sol-gel method also often produces non-uniform agglomerated  $\text{TiO}_2$  thus giving low activity<sup>10</sup>. This method also needs a long time for aging making this method less practice. Another method that allows using  $\text{TiO}_2$  powder which is obtainable and inexpensive is autoclave assisted hydrothermal method with moderate temperature and pressure<sup>24</sup>. In general, the hydrothermal method produces more active  $\text{TiO}_2$  that has a larger surface area and pore volume than the sol-gel method in the photooxidation process<sup>25</sup> and also in the photocatalytic degradation<sup>26</sup>.

The sulfur-doped  $\text{TiO}_2$  photocatalyst has been used in the photodegradation of a variety of organic pollutants, including rhodamine B<sup>11</sup>, trichloroethylene<sup>13</sup>, and phenol<sup>14</sup>. However, a lack of reports about Congo red photo-decolorization using  $\text{TiO}_2$ -S under visible light can be traced in the literature.

Under the circumstances, this current research addresses the sulfur-doped  $\text{TiO}_2$  using  $\text{TiO}_2$  powder and sulfuric acid with the hydrothermal method. The photocatalyst activity of the sulfur-doped  $\text{TiO}_2$  is examined for Congo red dye decolorization under visible light irradiation. Additionally, to obtain the best condition for the dye decolorization, several factors determining the decolorization efficiency including photocatalyst dosage, irradiation time, and solution pH are evaluated through a batch experiment.

## Experimental Section

### Materials and instruments

The materials used were  $\text{TiO}_2$  P25, sulfuric acid, Congo-red, hydrochloric acid, and sodium hydroxide purchased from Merck with analytical grade. A variety of instruments were used for the analysis and characterization including Fourier-Transform Infrared (FTIR) (Shimadzu Prestige 21), X-Ray

Diffractionmeter (XRD) (Shimadzu 6000), UV-Visible Spectrophotometer (Pharmaspec UV-1700) with additional Specular Reflectance UV-Visible Spectrophotometer (SRUV) (UV-1800 Series) accessories, UV-Visible Spectrophotometer (Analytik Jena), and Scanning Electron Microscopy and Energy Dispersive X-Ray (SEM-EDX) (Hitachi SU 3500 with Coating Hirachi MC1000 ION SPUTTER 15 mA 20s).

### Preparation of sulfur doped $\text{TiO}_2$ ( $\text{TiO}_2$ -S)

$\text{TiO}_2$  powder about 1 g suspended in water was mixed with 25 mL of 25 mmol/L sulfuric acid solution, then the mixture was stirred magnetically for 10 min to obtain a homogeneous mixture. Then the homogeneous mixture was placed in the autoclave and was heated at  $150^\circ\text{C}$  for 5 h. The doped photocatalyst in the autoclave was separated from the water and then dried at  $90^\circ\text{C}$  for 2h. The same procedure was repeated for sulfuric acid with 50 and 100 mmol/L of concentrations. Thereby the doped photocatalysts that have been prepared were noted as  $\text{TiO}_2$ -S(25),  $\text{TiO}_2$ -S(50), and  $\text{TiO}_2$ -S(100), respectively following the concentrations of the sulfuric acid introduced.

### Characterization of $\text{TiO}_2$ -S

In the characterization by Fourier Transform Infrared (FTIR), the samples were pelleted with KBr powder under high pressure. The FTIR spectra were scanned in the range of  $4000 - 400 \text{ cm}^{-1}$  of the wavenumbers. The XRD was operated under  $\text{Cu-K}\alpha$ , 40 kV of the potential energy, and 5 mA of the electric current for taking the photocatalyst XRD patterns in the range of  $10-80^\circ$  of the  $2\theta$  angles. The spectra of the SRUV of the photocatalyst were drawn in the range of the wavelength from 300 to 800 nm. The scanning electron microscope-EDX images were taken under an SEM microscope machine.

### Photocatalytic activity of TiO<sub>2</sub>-S

In a typical procedure, 50 mg of TiO<sub>2</sub>-S was added into 50 mL of the Congo-red solution with 10 mg/L of the concentration. Then the mixture was placed on the photo-process apparatus (Fig. 2) which was equipped with visible and UV lamps and magnetic stirring plates. The lamps were switched on to expose the light into the mixture along with constant stirring for the desired period. The solution then was filtered to separate it from the solid photocatalyst. Then the solution was analyzed by a visible spectrophotometer to find the left Congo red (undegraded) concentration. A decrease in the concentration of Congo red was determined by following Eq.1.

$$\frac{C_0 - C_t}{C_0} \times 100\% \quad \dots(1)$$

where E: The decreasing concentration of Congo red, C<sub>0</sub>: Initial concentration of the Congo red, and C<sub>t</sub>: Final concentration of the Congo red.

## Results and Discussion

### Characterization data

#### FTIR data

Characterization with FTIR is intended to confirm the occurrence of the S doping into TiO<sub>2</sub>. FTIR spectra of TiO<sub>2</sub> and the S doped TiO<sub>2</sub> with various S amounts are illustrated in Fig. 3. In the TiO<sub>2</sub> spectrum, the absorption bands are observed at 3425, 1635, 678, and 516 cm<sup>-1</sup>. The absorptions at 678 and 516 cm<sup>-1</sup> are contributed by O–Ti–O and Ti–O–Ti, respectively<sup>17</sup>. The absorption bands at 3425 and 1635 cm<sup>-1</sup> assign the presence of the O–H bond from water absorbed on the TiO<sub>2</sub> surface<sup>18</sup>.

In the spectra of the S doped TiO<sub>2</sub> with various amounts of S, the same peaks as the characteristic

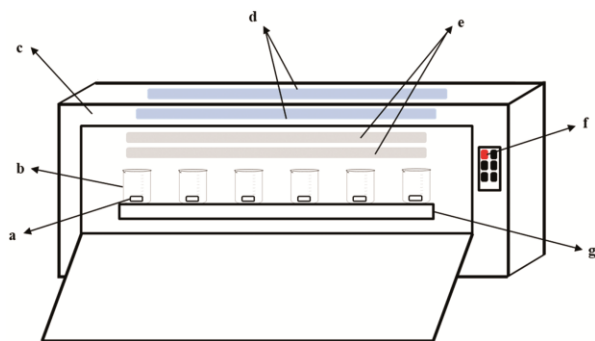


Fig. 2 — The apparatus for dye decolorization is composed of (a) magnetic stirrer bar, (b) sample solution, (c) melamine box, (d) UV lamps, (e) Visible lamps, (f) the switch and (g) magnetic stirrer plate

peaks belonging to TiO<sub>2</sub> are observed, with the new weak peaks located at 1041 and in 1087 - 1096 cm<sup>-1</sup>. These new peaks are related to the Ti–O–S and S =O bond vibrations<sup>14,19</sup>. Additionally, the shifts from 516 and 678 to 578 - 594 and 686 cm<sup>-1</sup> are also notified, signifying the interaction of the Ti–O–Ti and O–Ti–O bonds with S dopant atoms<sup>20</sup>. The appearance of some characteristic peaks suggests that S atoms have been successfully doped into TiO<sub>2</sub> crystal.

#### XRD data

The diffraction patterns of TiO<sub>2</sub> and S-doped TiO<sub>2</sub> are exhibited in Fig. 4. The characteristic peaks of TiO<sub>2</sub> are observable at 25,16°; 36,81°; 37,67°; 38,44°; 47,92°; 53,77°; 54,95°; and 62,58° of the 2θ values. This pattern is in agreement with TiO<sub>2</sub> anatase stated in COD No. 00-720-6075<sup>27</sup>.

The peaks in the XRD patterns of the S doped TiO<sub>2</sub> photocatalysts are seen similar to the pattern of TiO<sub>2</sub> without any new peaks of S dopant. It is indicated that the amount of S is very low and/or is present in the amorphous form. In addition, the doping S causes a decrease in the intensities of the XRD patterns, and the intensities are advanced to decline as the S loaded increases. The decrease in intensities notifies the crystallinity distortion due to the interaction between S and O–Ti–O lattice in TiO<sub>2</sub> crystal<sup>24</sup>.

#### SRUV data

The SRUV spectra of TiO<sub>2</sub> and TiO<sub>2</sub>-S with various S content are displayed in Fig. 5. Based on the spectra, the wavelength of the absorption edge was determined using the Tauc Plot method<sup>28</sup>. Further, the wavelengths obtained were used to determine the values of the band gap energy. The wavelengths and the band gap energy values are presented in Table 1.

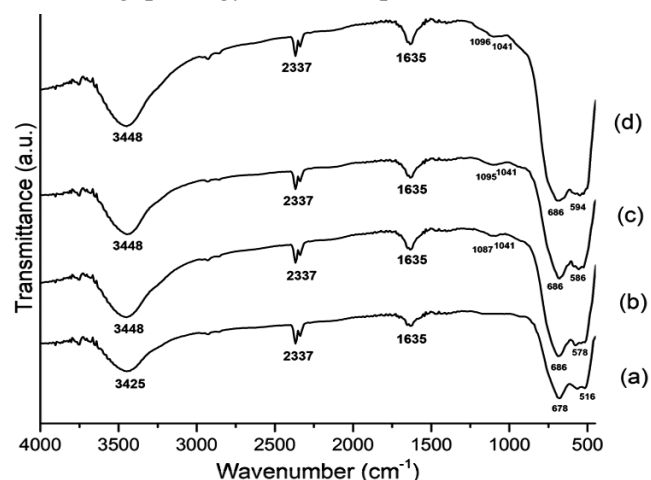


Fig. 3 — FTIR spectra of (a) TiO<sub>2</sub>, (b) TiO<sub>2</sub>-S(25), (c) TiO<sub>2</sub>-S(50), and (d) TiO<sub>2</sub>-S(100).

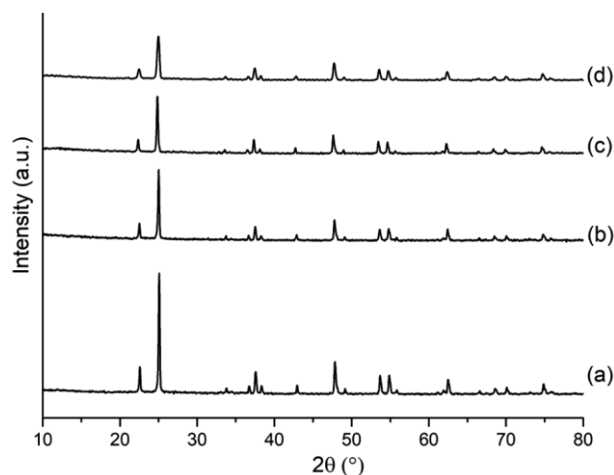


Fig. 4 — XRD diffraction patterns of (a)  $\text{TiO}_2$ , (b)  $\text{TiO}_2\text{-S}(25)$ , (c)  $\text{TiO}_2\text{-S}(50)$  and (d)  $\text{TiO}_2\text{-S}(100)$ .

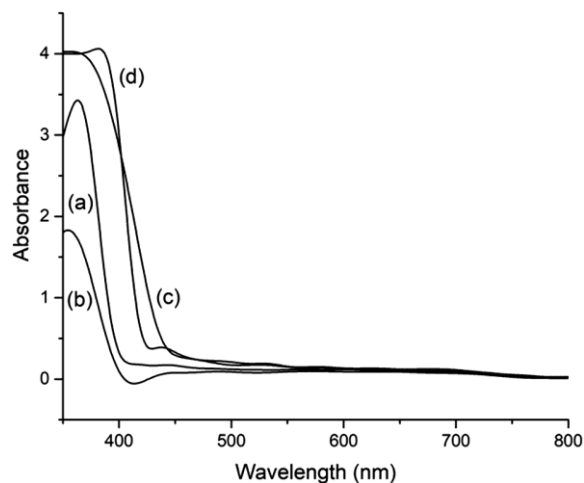


Fig. 5 — SRUV spectra of (a)  $\text{TiO}_2$ , (b)  $\text{TiO}_2\text{-S}(25)$ , (c)  $\text{TiO}_2\text{-S}(50)$ , and (d)  $\text{TiO}_2\text{-S}(100)$ .

Table 1 — Wavelength and band gap energy of the photocatalysts

| Material                         | $E_g$ (eV) | $\lambda$ (nm) |
|----------------------------------|------------|----------------|
| (a) $\text{TiO}_2$               | 3.20       | 387            |
| (b) $\text{TiO}_2\text{-S}(25)$  | 3.19       | 389            |
| (c) $\text{TiO}_2\text{-S}(50)$  | 2.92       | 425            |
| (d) $\text{TiO}_2\text{-S}(100)$ | 3.00       | 413            |

It is observed that light absorption of  $\text{TiO}_2\text{-S}$  samples shifts to the visible region, which decrease the  $E_g$  values. The decrease of  $E_g$  is caused by a narrowing gap due to the dopant insertion into the gap in the semiconductor structure of  $\text{TiO}_2$ <sup>16,21</sup>. The decrease of the  $E_g$  values is in line with the increase of S loaded, due to more S dopant being inserted<sup>29</sup>.

#### SEM images

The SEM images along with the EDX spectra for  $\text{TiO}_2$  and  $\text{TiO}_2\text{-S}(50)$  are presented in Fig. 6. The

appearance of  $\text{TiO}_2$  is spherical with ununiform size, while the surface of  $\text{TiO}_2\text{-S}$  particles is seen to be covered by the amorphous phase of the S dopant.

The EDX spectra of  $\text{TiO}_2$  present the main chemicals contained in the undoped and the S-doped  $\text{TiO}_2$ . The chemicals are presented in Table 2, showing that 0.3% of S is contained in the S doped  $\text{TiO}_2$  contents, while the element is not found in  $\text{TiO}_2$ . This data clearly attribute that S atoms have been doped in the  $\text{TiO}_2$  photocatalyst.

#### Photoactivity of $\text{TiO}_2\text{-S}$ in the dye decolorization

##### Effect of the S doping

The results of the dye photo-decolorization over the undoped and the S doped  $\text{TiO}_2$  under visible and UV irradiation is illustrated in Fig. 7. The Figure exhibited that doping S can increase the photocatalytic activity both in the presence of visible and UV lights. The increase of the activity of  $\text{TiO}_2\text{-S}$  under visible light is generated by the lower  $E_g$  allowing the  $\text{TiO}_2\text{-S}$  to be activated by visible light. The enhancement of  $\text{TiO}_2\text{-S}$  under UV light may be induced by the prevention of the electron and hole recombination. This is because the dopant can act as the separation center of the electron and hole pair, providing more holes and so more OH radicals can be provided<sup>30,31</sup>.

The dye photo-decolorization improves with the increase of the S loaded, but the opposite trend is observed when the amount of S doped was further increased. The excessive S dopant amount may be formed a larger aggregate covering the surface of  $\text{TiO}_2$  that can reduce the contact of the light with the  $\text{TiO}_2$ . This can result in fewer OH radicals, hence the less efficient photodecolorization<sup>30,32</sup>.

##### Effect of the irradiation time

The effect of the irradiation time on the photo-decolorization of the dye is shown in Fig. 8(a). Notably, the extension time up to 60 min results in higher photo-decolorization, but the irradiation longer than 60 min gives no effect on the decolorization. It is indicated that the irradiation time is longer than 60 min, and the OH radical formation has reached saturation level.

##### Effect of the photocatalyst mass

The photo-decolorization results from various doses of the photocatalyst are exhibited in Fig. 8(b). The photo-decolorization is seen to rise with the increase of the photocatalyst mass, however, a negative effect is observable for the further increase

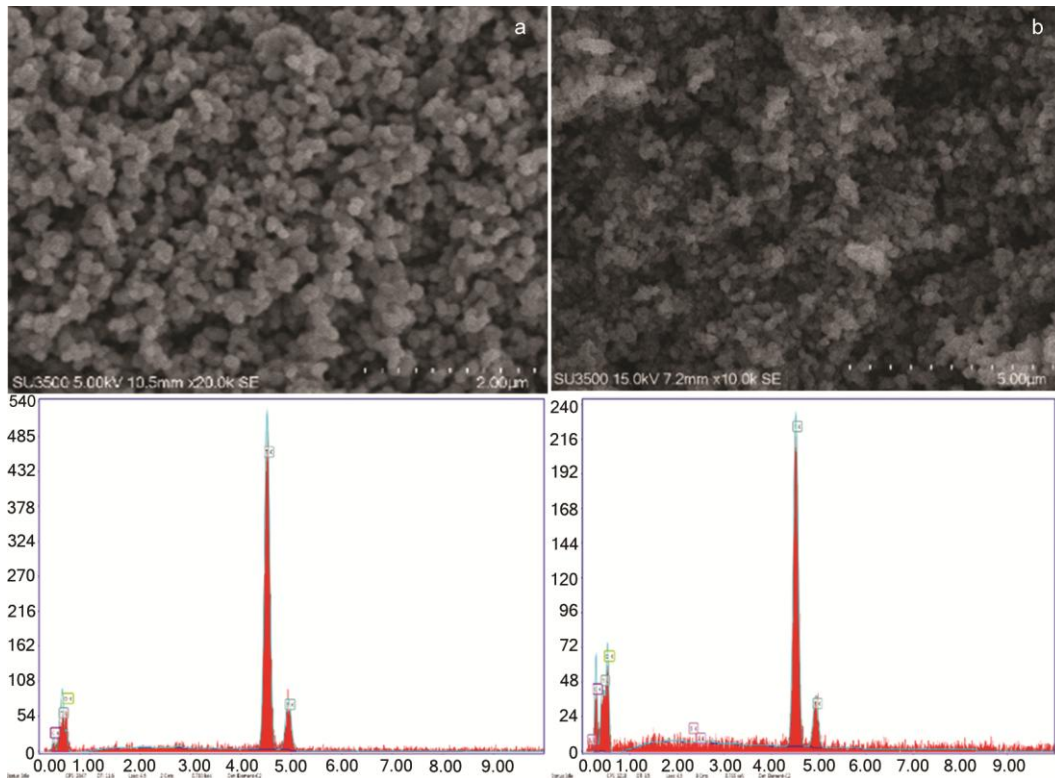


Fig. 6 — SEM-EDX spectra of (a) TiO<sub>2</sub>, and (b) TiO<sub>2</sub>-S(50)

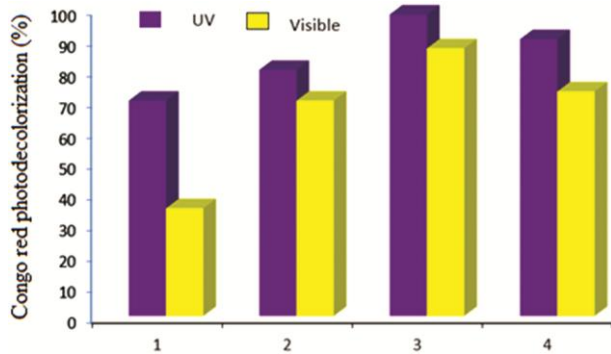


Fig. 7 —Effect of S doping into TiO<sub>2</sub> of photo-decolorization on the Congo red photo-decolorization under UV and visible lights of 1) TiO<sub>2</sub>, 2) TiO<sub>2</sub>-S(25), 3) TiO<sub>2</sub>-S(50), and 4) TiO<sub>2</sub>-S(100).

of the photocatalyst dose. The photocatalyst dose represents the number of OH radicals. The photocatalyst exceeding the optimum level can increase the turbidity of the media that inhibits the light penetration, thereby declining the availability of the OH radicals<sup>16,32</sup>.

**Effect of the solution pH**

Figure 8(c) displays the effect of pH on dye photo-decolorization. It is assigned the slight increase of the

Table 2 — Chemical composition of the TiO<sub>2</sub> and TiO<sub>2</sub>-S based on the SEM-EDX

| Element | % Mass           |                               |
|---------|------------------|-------------------------------|
|         | TiO <sub>2</sub> | Sulfur doped TiO <sub>2</sub> |
| C       | 5.4              | 6.5                           |
| O       | 43.7             | 44.8                          |
| Ti      | 50.9             | 48.4                          |
| S       | -                | 0.3                           |
| Total   | 100              | 100                           |

Decolorization when the pH was increased up to 6 and the decolorization diminishes drastically at higher pH than 8. The *pH<sub>zpc</sub>* of TiO<sub>2</sub> is about 6.5<sup>33</sup>. At very low pH, both TiO<sub>2</sub> and Congo-red tends to have positive charges, restricting TiO<sub>2</sub> to adsorb the dye, so reducing the number of the dye to be degraded. Increasing pH from 2 – 8 has produced more decolorization since the Congo-red tends to be neutral molecules and the positive charged TiO<sub>2</sub> still existed. This allows more dye to be adsorbed<sup>34</sup>. The occurrence of the sharp decrease of the photo-decolorization in the pH higher than 8, is due to the repulsion of the dye and TiO<sub>2</sub> interaction. In the pH range, the negative charges of TiO<sub>2</sub> as well as the dye increase<sup>31</sup>.

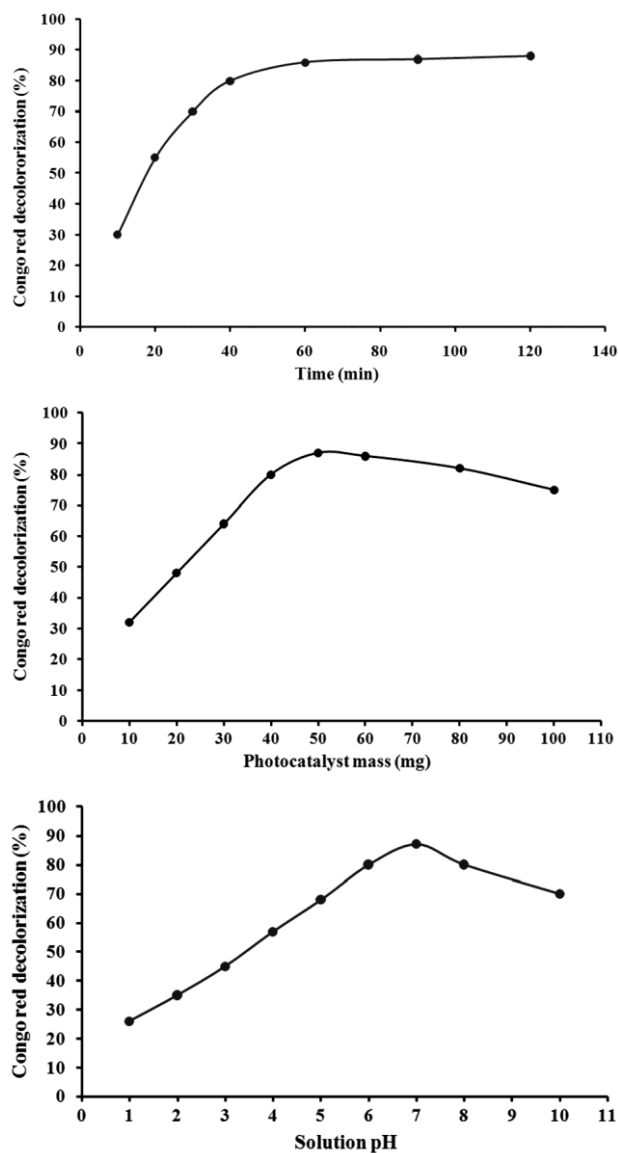


Fig. 8 — (a) Effect of the reaction time on the photo-decolorization of Congo red over TiO<sub>2</sub>S(50); (b) Effect of the photocatalyst mass on the photo-decolorization of Congo red over TiO<sub>2</sub>-S(50); (c) Effect of pH on the photo-decolorization of Congo red over TiO<sub>2</sub>-S(50)

## Conclusion

It can be concluded that doping S atoms from H<sub>2</sub>SO<sub>4</sub> solutions with various concentrations (25, 50, and 100 mmol/L) into TiO<sub>2</sub> structure have been successfully conducted that was able to decrease the band gap energy (E<sub>g</sub>) into the visible region and thereby enhance its activity under visible light. The most effective decreasing E<sub>g</sub> and enhancing activity under visible light was observed for TiO<sub>2</sub>-S prepared from 50 mmol/L of H<sub>2</sub>SO<sub>4</sub>. The effectiveness of the visible photo-decolorization of Congo red over S

doped TiO<sub>2</sub> was found to be controlled by photocatalyst mass, reaction time, and solution pH, and the highest decolorization of Congo red 10 mg/L in 50 mL solution, which was around 87%, could be reached by applying 50 mg of the photocatalyst mass, in 60 min and at pH 7.

## Acknowledgements

A great appreciation to the Director of Research and Community Service at Gadjah Mada University for the financial support through a Research Grant of Final Project Recognition (RTA) 2020.

## References

- Liu X, Li W, Chen N, Xing X, Dong C & Wang Y, *RSC Adv*, 5 (2015) 34456.
- Ho W, Yu J C & Lee S, *J Solid State Chem*, 179 (2006) 1171.
- Burda C, Lou Y, Chen X, Samia A C S, Stout J & Gole J L, *Nano Lett*, 3 (2003) 1049.
- Ali N, Said A, Ali F, Raziq F, Ali Z, Bilal M, Reinert L, Begum T & Iqbal H M N, *Water Air Soil Pollut*, 231 (2020) 1.
- Mayoufi A, Nsib M F & Houas, *Comptes Rendus Chim*, 17 (2014) 818.
- Sulaiman S N A, Noh M Z, Adnan N N, Bidin N & Ab Razak S N, *J Phys Conf Ser*, 1027 (2018) 1.
- Piátkowska A, Janus M, Szymański K & Mozia S, *Catalysts*, 11 (2021) 1.
- Madarász J, Brăileanu A, Crişan M, Răileanu M & Pokol G, *J Therm Anal Calorim*, 97 (2009) 265.
- Mahshid S, Askari M & Ghamsari M S, *J Mater Process Technol*, 189 (2007) 296.
- Nguyen T L, Quoc D V, Nguyen T L, Le T T T, Dinh T K, Nguyen V T & Nguyen P H, *J Nanomater*, 2021 (2021) 1.
- Lin Y H, Hsueh H T, Chang C W & Chu H, *Appl Catal B Environ*, 199 (2016) 1.
- Nishikiori H, Hayashibe M & Fujii T, *Catalysts*, 3 (2013) 363.
- Devi L G & Kavitha R, *Modification Mater Chem Phys*, 143 (2014) 1300.
- Lestari N D, Wahyuni E T & Aprilita N H, *Iran J Chem Chem Eng*, 40 (2021) 866.
- McManamon C, O'Connell J, Delaney P, Rasappa S, Holmes J D & Morris M A, *J Mol Catal A Chem*, 406 (2015) 51.
- Dodoo-Arhin D, Buabeng F P, Mwabora J M, Amaniampong P N, Agbe H, Nyankson E, Obada D O & Asiedu N Y, *Heliyon*, 4 (2018) 1.
- Shapovalova M V, Khalyavka T A, Shcherban N D, Khyzhun O Y, Permyakov V V & Shcherbakov S N, *Nanosystems Nanomater Nanotechnol*, 18 (2020) 681.
- Ivanov S, Barylyak A, Besaha K, Bund A, Bobitski Y, Wojnarowska-Nowak R, Yaremchuk I & Kus-Liśkiewicz M, *Nanoscale Res Lett*, 11 (2016) 1.
- Kavitha V, *Int J Recent Sci Res*, 10 (2019) 33763.
- Ohno T, Mitsui T & Matsumura M, *Chem Lett*, 32 (2004) 364.

- 21 Rezaee M, Mousavi Khoie S M & Liu K H, *Cryst Eng Comm*, 13 (2011) 5055.
- 22 Makuła P, Pacia M & Macyk W, *J Phys Chem Lett*, 9 (2018) 6814.
- 23 Mahy J G, Cerfontaine V, Poelman D, Devred F, Gaigneaux E M, Heinrichs B & Lambert S D, *Materials*, 11 (2018) 1.
- 24 Mattsson A, Lejon C, Bakardjieva S, Štengl V & Österlund L, *J Solid State Chem*, 199 (2013) 212.
- 25 Bakar S A & Ribeiro C A, *J Mol Catal A Chem*, 421 (2016) 1.
- 26 Wang F, Ban P P, Parry J P, Xu X H & Zeng H, *Rare Met*, 35 (2016) 940.
- 27 Khan H, Swati I K, Younas M & Ullah A, *Int J Photoenergy*, 2017 (2017) 1.
- 28 Zeng M, *Bull Korean Chem Soc*, 34 (2013) 953.
- 29 Hua L, Yin Z & Cao S, *Catalysts*, 10 (2020) 1.